ISSN 1063-7842, Technical Physics, 2015, Vol. 60, No. 4, pp. 541–545. © Pleiades Publishing, Ltd., 2015.
Original Russian Text © A.O. Sel'skii, A.A. Koronovskii, O.I. Moskalenko, A.E. Hramov, T.M. Fromhold, M.T. Greenaway, A.G. Balanov, 2015, published in Zhurnal Tekhnicheskoi Fiziki, 2015, Vol. 85, No. 4, pp. 62–66.

Effect of Interminiband Tunneling on the Generation of Current in a Semiconducting Superlattice

A. O. Sel'skii[a, b], A. A. Koronovskii[a, b], O. I. Moskalenko[a, b], A. E. Hramov[a, b], T. M. Fromhold[c], M. T. Greenaway[c], and A. G. Balanov[b, d]

[a] *Gagarin State Technical University, Politekhnicheskaya ul. 77, Saratov, 410056 Russia*
[b] *Chernyshevskii State University, Astrakhanskaya ul. 83, Saratov, 410012 Russia*
[c] *School of Physics and Astronomy, University of Nottingham, Nottingham, NG7 2RD UK*
[d] *Department of Physics, Loughborough University, Loughborough, LE11 3TU UK*
e-mail: feanorberserk@gmail.com

Received November 7, 2013

Abstract—The effect of the bandgap width between the first and second energy minibands on the charge transport in a semiconducting superlattice to which electric and tilted magnetic fields are applied is studied theoretically. The time dependences of the current passing through the superlattice are calculated, and the dependences of the amplitude and frequency of electric current oscillations on the applied voltage are constructed. It is found that the interminiband electron tunneling facilitates a decrease in the amplitude of current oscillations, but simultaneously increases their frequency.

DOI: 10.1134/S1063784215040246

Semiconducting superlattices are complex nanostructures consisting of several alternating thin (~10 nm) layers of various semiconducting materials that usually have close crystal lattice periods (e.g., GaAs and AlGaAs) [1, 2]. The difference in the bandgap widths of such materials ensures the spatially periodic modulation of the conduction band, which leads to the formation of narrow energy minibands for charges moving in the direction perpendicular to the surface of the layer [3, 4]. In the presence of a static electric field, these specifically quantum-mechanical properties of the semiconducting superlattice make possible the emergence of Bloch oscillations localizing electrons and, hence, leading to the formation of a descending segment on the current–voltage characteristic of the device. Under the conditions of a negative differential conductivity, a semiconducting superlattice can generate current oscillations associated with the drift of domains with a high charge concentration. It was shown experimentally that the frequency of oscillations of the current passing through the semiconducting superlattice may attain values on the order of 100 GHz [5, 6]. The motion of domains in the superlattice can be controlled by a tilted magnetic field [7, 8]; complex trajectories of individual electrons appearing in this case [9–11] may significantly improve the amplitude and frequency characteristics of the current being generated [7, 12].

In simulating and constructing strongly coupled superlattices, the spacing between minibands is usually set to be large enough to disregard the Landau–Zener interminiband tunneling [7, 9, 10, 12, 13]. In this case, the description of charge transport in superlattices, as well as the interpretation of experimental data, is simplified significantly. However, the effect of the interband tunneling on the amplitude and frequency characteristics of superlattices remains an important fundamental problem interesting for technical applications. This effect has been studied insufficiently and calls for systematic analysis.

In this study, we describe the results of computer simulation of the dynamics of electric current passing through a semiconducting superlattice for various values of bandgap width E_g between the first and second energy minibands. In particular, we construct the dependences of frequencies and amplitudes of electric current oscillations in the semiconducting superlattice in crossed electric and magnetic fields for various values of the bandgap width.

The simulation of processes occurring in the semiconducting superlattice was based on the system of equations including the continuity equation, the Poisson equation, and the expression for the current density taking into account the electron drift velocity [2, 7]:

$$
\begin{gathered}
e\frac{\partial n}{\partial t} = \frac{\partial J}{\partial x}, \\
\frac{\partial F}{\partial x} = \frac{e}{\varepsilon_0 \varepsilon_r}(n - n_D), \qquad (1) \\
J = en v_d(\mathbf{F}),
\end{gathered}
$$

where t denotes time and coordinate x corresponds to the direction perpendicular to the layers of the superlattice. Variables $n(x, t)$, $F(x, t)$, and $J(x, t)$ determine

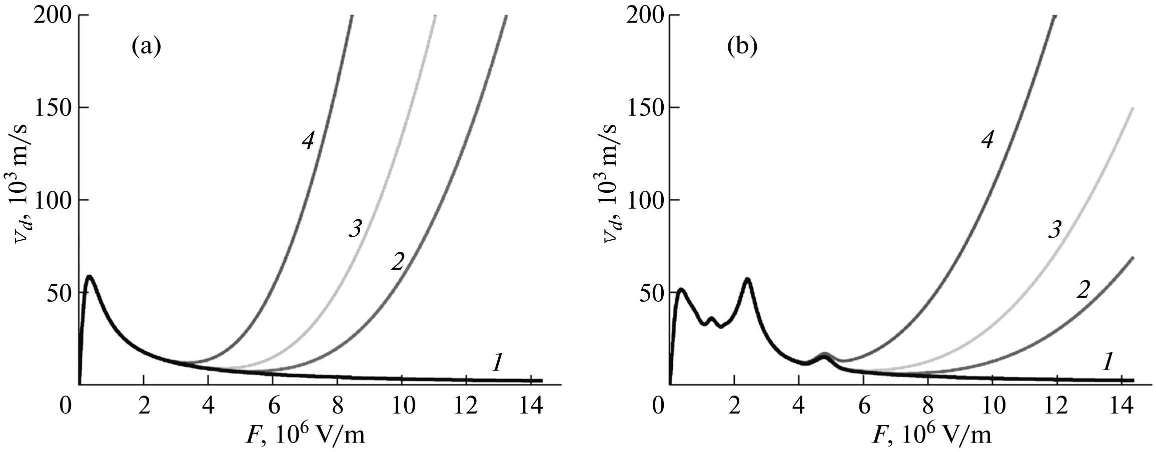

Fig. 1. Dependences of the electron drift velocities on the electric field strength for various gap widths between the first and second energy minibands: (a) in zero magnetic field (b) in a tilted magnetic field, $B = 15$ T, $\theta = 40°$; curve *1* corresponds to the absence of tunneling; (*2*) $E_g = 150$; (*3*) 133, and (*4*) 111 meV.

the concentration, electric field strength, and current density, respectively. Parameters ε_0 and ε_r are the absolute and relative permittivity, respectively; n_D is the equilibrium concentration of electrons; v_d is the electron drift velocity calculated for mean value of $\mathbf{F}$, and e is the electron charge.

Following [8, 11], we assume that the contacts on the emitter and collector of the superlattice are Ohmic; in this case, current density J_0 through the emitter is determined by the conductivity $\sigma = 3788$ S of the contact, $J_0 = \sigma F(0)$, and electric field strength $F(0)$ can be determined from the boundary conditions

$$V = U + \int_0^L F(x)dx,$$

where V is the voltage applied to the superlattice and U is the voltage drop across the contact [8].

For zero magnetic field, the dependence of the drift velocity on the electric field strength at low temperatures can be calculated analytically using the Esaki and Tsu formula [4]

$$v_d = \frac{\Delta d}{2\hbar}\frac{\omega_B\tau}{(\omega_B\tau)^2+1}, \tag{2}$$

where Δ is the width of the first miniband, d is the superlattice period, τ is the effective electron scattering time, and $\omega_B = eFd/\hbar$ is the frequency of Bloch oscillations. In the presence of a tilted electric field, the dependence of the drift velocity on the electric field strength was calculated numerically using the semiclassical theory described in detail in [5, 10, 11]. The possibility of tunneling between the first and second minibands was taken into account using the approach described in [14, 15]. In this approach, the drift velocity with allowance to interminiband tunneling is defined as

$$v_{d,\,\mathrm{mod}} = v_d(1-T(F)) + T(F)v_{d,\,\mathrm{free}}, \tag{3}$$

$$v_{d,\,\mathrm{free}} = \frac{eF\tau}{2m^*}(\cos\theta)^2, \tag{4}$$

where m^* is the effective mass of an electron in the semiconductor and θ is the magnetic field tilt angle relative to the x axis. In this case, $v_{d,\,\mathrm{free}}$ is the drift velocity of the electron in the second miniband, calculated in the free electron approximation. Interminiband tunneling probability $T(F)$ is defined in accordance with [14–16] as

$$T(F) = \exp\left(\frac{m^*d(E_g)^2}{4\hbar^2|eF|\cos\theta}\right), \tag{5}$$

where E_g is the bandgap width between the first and second minibands. The presence of cosines in expressions (4) and (5) reflects the presence of a tilted magnetic field applied at angle θ relative to the superconducting superlattice.

In our simulation, we used the following values of parameters describing actual devices used in experiments [10, 12]: $m^* = 0.067m_e$, where m_e is the mass of a free electron; $\Delta = 19.1$ meV, $d = 8.3$ nm, $\tau = 0.25$ ps, $n_D = 3 \times 10^{22}$ m^{-3}, $\varepsilon_r = 12.5$, magnetic induction is $B = 15$ T, and $\theta = 40°$.

Figure 1a shows the dependence of drift velocities on the electric field strength for various values of E_g in zero magnetic field. In this case, the peak corresponding to the maximal electron drift velocity, which remains unchanged for any E_g, can be observed. It can be seen from formula (2) that this peak, which will be henceforth referred to Esaki–Tsu peak [4], appears when $\omega_B\tau = 1$, which corresponds to stabilization of Bloch oscillations. With increasing electric field strength F, the number of Bloch oscillations performed by an electron between scattering events increases, which leads to a decrease in the drift veloc-

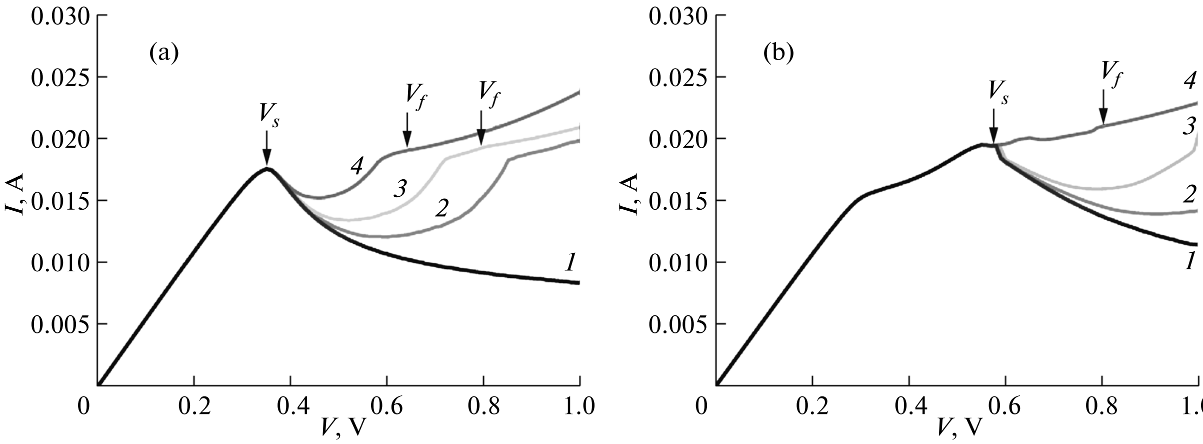

Fig. 2. Current–voltage characteristics for various values of the gap width between the first and second energy minibands: (a) in zero magnetic field (b) in a tilted magnetic field, $B = 15$ T, $\theta = 40°$; curve *1* corresponds to the absence of tunneling; (*2*) $E_g = 150$; (*3*) 133, and (*4*) 111 meV. Arrows mark the values of V corresponding to the emergence (V_s) and failure (V_f) of current oscillations.

ity. A further increase in F substantially increases the interminiband tunneling probability, which in turn leads to a sharp increase in the electron drift velocity. With decreasing E_g, the value of F at which the electron drift velocity begins to increase as a result of interminiband tunneling obviously also decreases.

In a tilted magnetic field, the dependence of the drift velocity on the electric field strength (see Fig. 1b) acquires other peaks also apart from the Esaki–Tsu peak. These peaks appear due to resonances of oscillations at the Bloch frequency ω_B and cyclotron frequency $\omega_c = eB\cos\theta/m^*$, which correspond to ratios $\omega_B/\omega_c = 0.5$, 1, and 2 [9, 11]. In the presence of the tilted magnetic field, the drift velocity in the range of strong electric fields also increases. Like in zero magnetic field, this effect can be explained by the fact that the electron mobility in the second miniband to which the electron is tunneling is higher than in the first miniband.

Figure 2a shows the current–voltage characteristics calculated for different values of the bandgap width E_g between the first and second minibands in zero magnetic field. Figure 2b represents the current–voltage characteristic in the case when a tilted magnetic field is applied to the superlattice. In both cases, at the onset of generation (V_S), the I–V characteristic acquires a noticeable descending segment on which the differential resistance is negative.

For finite values of E_g (curves *2–4*), upon an increase in voltage, the descending segment on the I–V curve changes for a segment with increasing current. This can be due to the fact that with increasing V, the values of electric field strength become sufficient for inducing interminiband tunneling and, hence, for increasing the electron drift velocity (see Fig. 1). Upon a further increase in V, this region expands, and for a large V (V_f in Fig. 2), failure of current oscillations takes place.

Figure 3a shows the dependences of current oscillation amplitude ΔI on voltage V in zero magnetic field. It can be seen that for a finite gap width, there exists a finite range of V values in which the current passing through the superlattice exhibits oscillations (Figs. 3c and 3d show examples of the time dependence of current for $V = 0.8$ V and $E_g = 150$ meV). The form of such dependences changes when a tilted magnetic field is applied to the superlattice (Figs. 3b, 3d). It can be seen that the magnetic field shifts the current oscillation threshold towards higher values of V (cf. Figs. 3a and 3b). Like in zero magnetic field, the finite gap width limits the oscillation generation region. In addition, the application of the magnetic field complicates the $\Delta I(V)$ dependence, which acquires several local peaks (see curve *4* in Fig. 3b). The magnetic field also changes the form of current oscillations in the semiconducting superlattice for the same values of control parameters. For example, for $V = 0.8$ V and $E_g = 150$ meV (Figs. 3c, 3d), the magnetic field substantially increases the amplitude of oscillations (the frequency of oscillations also changes thereby, although this change is not so strong for the values of V and E_g used in Figs. 3c and 3d).

Figure 4 illustrates the dependence of frequency f of current oscillations on applied voltage V for various values of E_g in zero (Fig. 4a) and nonzero (Fig. 4b) tilted magnetic fields. In both cases, a decrease in the gap width leads to an increase in the domain repetition rate. This is due to the fact that interminiband tunneling reduces the electron concentration in the drifting charge domain. The formation of a moving domain is associated with the descending segment on the $v_d(F)$ curve (see Fig. 1) [7], for which a higher value of F indicates a lower electron drift velocity v_d. Thus, a decrease in the charge concentration in a domain reduces the local electric field strength, leading to acceleration of electrons in the domain and to an

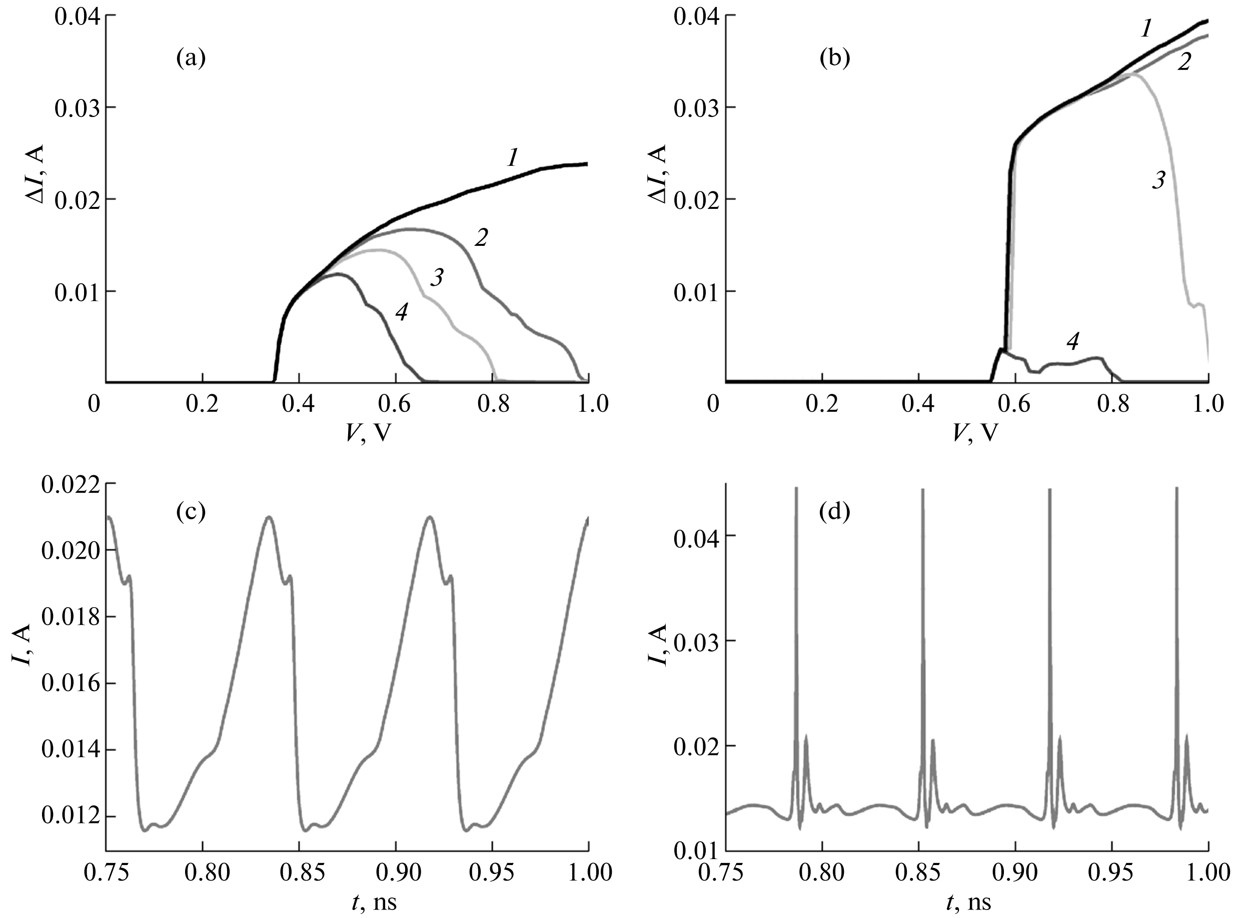

Fig. 3. Dependences of the electric current oscillations on the voltage applied to the semiconducting superlattice for various gap widths between the first and second energy minibands: (a) in zero magnetic field (b) in a tilted magnetic field, $B = 15$ T, $\theta = 40°$; curve *1* corresponds to the absence of tunneling; (*2*) $E_g = 150$; (*3*) 133, and (*4*) 111 meV; time realizations of current for $V = 0.8$ V and $E_g = 150$ meV (c) in zero magnetic field and (d) in a tilted magnetic field $B = 15$ T, $\theta = 40°$.

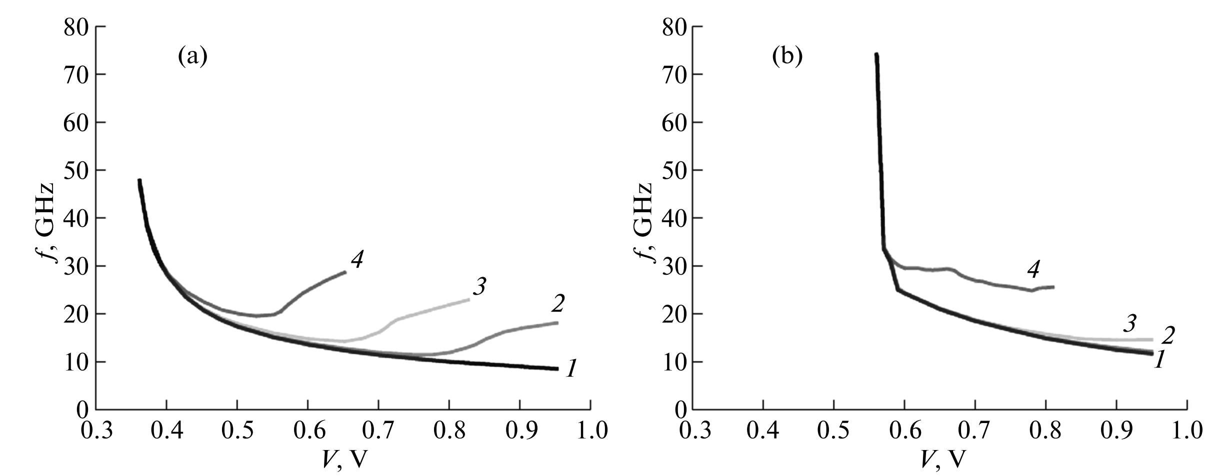

Fig. 4. Dependence of the frequency of electric field oscillations on the voltage applied to the semiconducting superlattice for various values of the gap width between the first and second minibands: (a) in zero magnetic field (b) in a tilted magnetic field, $B = 15$ T, $\theta = 40°$; curve *1* corresponds to the absence of tunneling; (*2*) $E_g = 150$; (*3*) 133, and (*4*) 111 meV.

increase in the frequency of oscillations. At the same time, it can be seen that while the presence of a magnetic field in the absence of tunneling increases the frequency for any values of V, the effect of the magnetic field on the frequency of current oscillations for finite values of E_g depends on the applied voltage. For low voltages V, the magnetic field increases the current oscillation frequency, while in the range of relatively high voltages, the frequency of oscillations in a nonzero magnetic field may decrease (Figs. 4a, 4b, curves *2*, *3*).

Thus, it has been established that interminiband tunneling of electrons in a semiconducting superlattice may noticeably affect the amplitude and frequency characteristics of current oscillations being generated. In particular, a decrease in the gap width between the first and second minibands may lead to a decrease in the amplitude of current oscillations, while the frequency of oscillations may noticeably increase. These effects are preserved in the presence of a tilted magnetic field and can be used in designing devices on the basis of semiconducting superlattices. The nature of these phenomena is explained by the influence of the interminiband tunneling on the charge concentration in moving domains; however, further investigations are required for obtaining a comprehensive explanation of the mechanisms of these effects.

ACKNOWLEDGMENTS

This study was financed by the Ministry of Education and Science of the Russian Federation (assignment nos. 3.23.2014/K and 931), by the Grant Council of the President of the Russian Federation for supporting leading scientific schools (project no. NSh-828.2014.2), the Russian Foundation for Basic Research (project no. 15-32-20299), and the Dynasty foundation for noncommercial programs.

REFERENCES

1. A. Ya. Shik, Sov. Phys. Semicond. **8**, 1195 (1974).
2. A. Wacker, Phys. Rep. **357**, 1 (2002).
3. L. V. Keldysh, Fiz. Tverd. Tela (Leningrad) **4**, 2265 (1962).
4. L. Esaki and R. Tsu, IBM J. Res. Dev. **14**, 61 (1970).
5. R. Scheuerer, E. Schomburg, K. F. Renk, et al., Appl. Phys. Lett. **81**, 1515 (2002).
6. H. Eisele, S. P. Khanna, and E. H. Lineld, Appl. Phys. Lett. **85**, 072101 (2010).
7. M. T. Greenaway, A. G. Balanov, E. Schöll, et al., Phys. Rev. B **80**, 205318 (2009).
8. A. G. Balanov, M. T. Grinavei, A. A. Koronovskii, et al., JETP **114**, 836 (2012).
9. T. M. Fromhold, A. A. Krokhin, C. R. Tench, et al., Phys. Rev. Lett. **87**, 046803 (2001).
10. T. M. Fromhold, A. Patanè, S. Bujkiewicz, et al., Nature **428**, 726 (2004).
11. A. O. Selskii, A. A. Koronovskii, A. E. Hramov, et al., Phys. Rev. B **84**, 235311 (2011).
12. N. Alexeeva, M. T. Greenaway, A. G. Balanov, et al., Phys. Rev. Lett. **109**, 024102 (2012).
13. E. Schomburg, T. Blomeier, K. Hofbeck, et al., Phys. Rev. B **58**, 4035 (1998).
14. D. P. A. Hardwick, S. L. Naylor, S. Bujkiewicz, et al., Physica E **32**, 1 (2006).
15. D. P. A. Hardwick, *Quantum and Semiclassical Calculations of Electron Transport through a Stochastic System*, PhD Thesis (Nottingham Univ., Nottingham, 2007).
16. C. Zener, Proc. R. Soc. London, Ser. A **145**, 523 (1934).

Translated by N. Wadhwa